Deep Spatial Profiling of Head and Neck Squamous Cell Carcinoma Offers Insights into the Tumor Microenvironment of HPV-Stratified Patients

Ettai Markovits[1], Hailing Zong[2], Pinchas Birnbaum[1], Becky Arbiv[1], Yuval Shachaf[1], Shai Bookstein[1], Ron Elran[1], Avi Laniado[1], Gali Golan[1], Kenneth J Bloom[1], Lauri Diehl[2], Abhishek Aggarwal[2]

[1]Nucleai, Israel; [2]Pathobiology, Gilead Sciences, Inc, United States of America

Conclusions

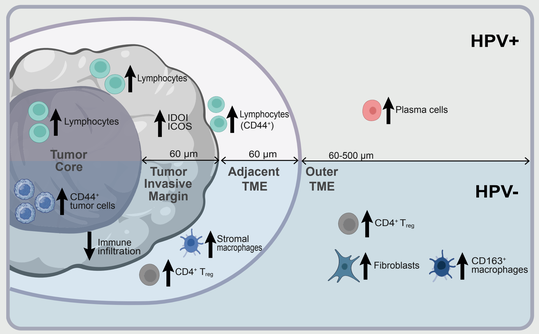

- Deep spatial analysis unveiled significant differences in the tumor microenvironment of HPV+ and HPV- HNSCC tumors
- Enrichment of lymphocytic infiltrates with elevated expression of inhibitory immune checkpoints in the tumor and TME of HPV+ patients, suggests potential benefits from immune checkpoint combinations
- Conversely, HPV− patients exhibited a higher proportion of stromal and suppressive myeloid cells in their TME, indicating potential benefits from targeting these cell types

Background

- Head and neck squamous cell carcinoma (HNSCC) is an aggressive, biologically heterogeneous disease that can arise in the oral cavity, oropharynx, hypopharynx, and larynx
  - Seventh most common cancer globally (roughly 4.5% of all cancer diagnoses around the world)
  - Estimated 890,000 new cases and 450,000 deaths per year
- Human papillomavirus (HPV) is a major risk factor for HNSCC development and HPV status correlates with prognosis and aids in the selection of optimal therapy
- While HPV-positive (HPV+) HNSCC patients have a better prognosis, compared with HPV-negative (HPV−), the mechanism underlying this improvement is unknown

Objective

- To employ a deep learning multiplex immunofluorescence (mIF) pipeline to assess cellular and spatial differences between HPV− and HPV+ HNSCC tumors

References:

[1]Markovits, E. et al. bioRxiv 2022.11.09.515776 (2022)

Disclosures:

DOI: AA is an employee of Gilead Sciences and holds stocks in the company.

Funding: Study sponsored by Gilead Sciences

Correspondence: Abhishek Aggarwal, **abhishek.aggarwal5@gilead.com**

Methods

- We profiled 16 HNSCC biopsies (7 HPV+ and 9 HPV− samples) with a 37-plex mIF panel (**Figure 1A**) and a corresponding H&E slide
- The panel consisted of core immune cell markers, immune activation status markers, as well as structural markers (**Figure 1B**)

Figure 1. PhenoCycler™-Fusion Workflow and Antibody Panel

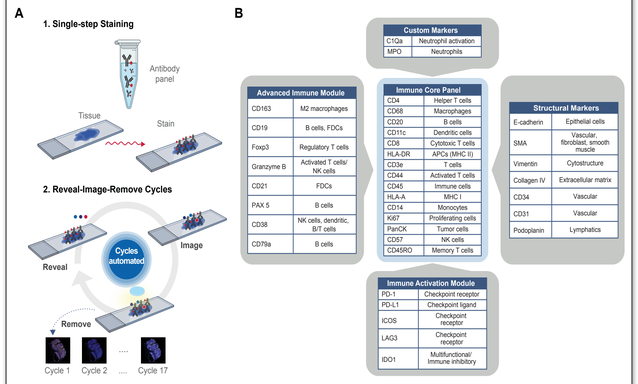

(A) Steps outlined showcasing the staining and imaging workflow. (B) Composition of the 37-plex antibody panel.

- Employing a deep learning mIF analysis pipeline (**Figure 2**), cells were segmented, and marker positivity was determined by a deep learning-based classifier
- For area segmentation, we employed a deep learning-based area model transferred from the corresponding H&E image. Each slide was segmented into tumor and stromal areas:
  - **Tumor core**
  - **Tumor invasive margin** (the outer 60 µm rim of the tumor)
  - **Adjacent tumor microenvironment** (60 µm rim from the tumor-stroma border)
  - **Outer tumor microenvironment** (60-500 µm rim from the tumor-stroma border)
- Tertiary lymphoid structures were identified based on T-cell and B-cell aggregates with CD21+
- Spatial features were calculated based on area assignment, cell types and phenotypic markers
- Cell distribution between areas and differential expression of spatial features were compared using Mann-Whitney U test between HPV+ and HPV− samples

Figure 2. Deep-Learning-Based Image Analysis Workflow

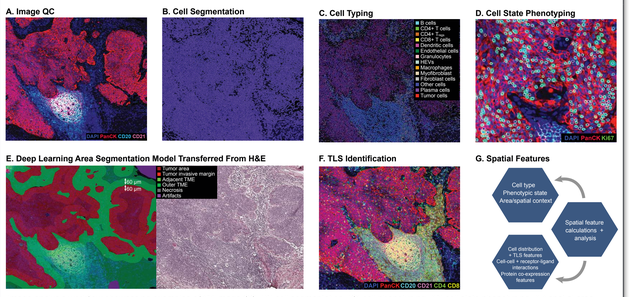

Image analysis workflow showcasing examples of (A) image QC, (B) cell segmentation, (C) cell phenotyping, (D) cell state phenotyping, (E) spatial area allocation, (F) TLS identification, and (G) possible spatial features that can be derived analytically.

Results

Figure 3. High-Resolution Imaging of Biomarkers on HNSCC Tumors

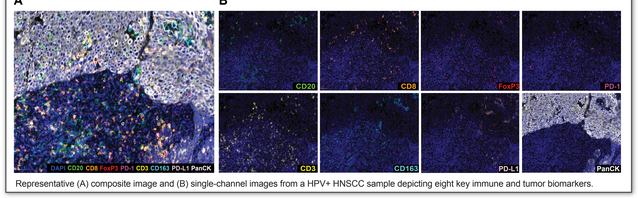

Representative (A) composite image and (B) single-channel images from a HPV+ HNSCC sample depicting eight key immune and tumor biomarkers.

Results

Performance evaluation of cell typing

- Utilizing marker positivity prediction, 14 distinct cell types were identified based on known lineage marker expression
- Performance evaluation in manual annotations demonstrated balanced accuracy above 85% in 13/14 cell types and a F1-score above 75% in 12/14 cell types (**Figure 4**)

Figure 4. Cell-Typing Model Performance

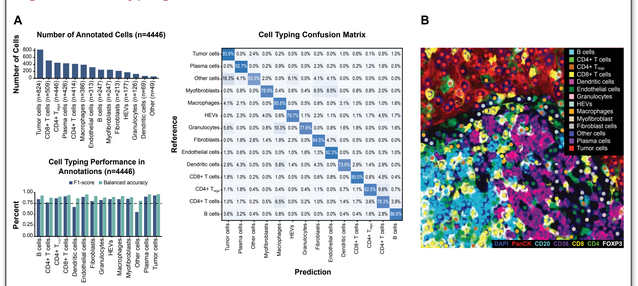

(A) Cell-typing performance evaluation against manual cell-type annotations. (B) Representative image demonstrating cell-type identification within the tissue.

Differential cell-type fraction within areas in HPV+ and HPV− tumors

- We observed a higher abundance of T cells (CD8+, CD4+ and CD4+ T_{regs}) and B cells in the tumor invasive margin of HPV+ tumors. Interestingly, all of these cell types were also more abundant in the adjacent TME, except for CD4+ T_{regs} that were also abundant in the HPV− tumors
- HPV− tumors demonstrated higher fractions of stromal cells (fibroblast, myofibroblasts, and endothelial cells) across the tumor invasive margin and TME, as well as a higher fraction of macrophages in the TME

Figure 5. Differential Spatial Abundance of Immune Cells Stratified by HPV Status

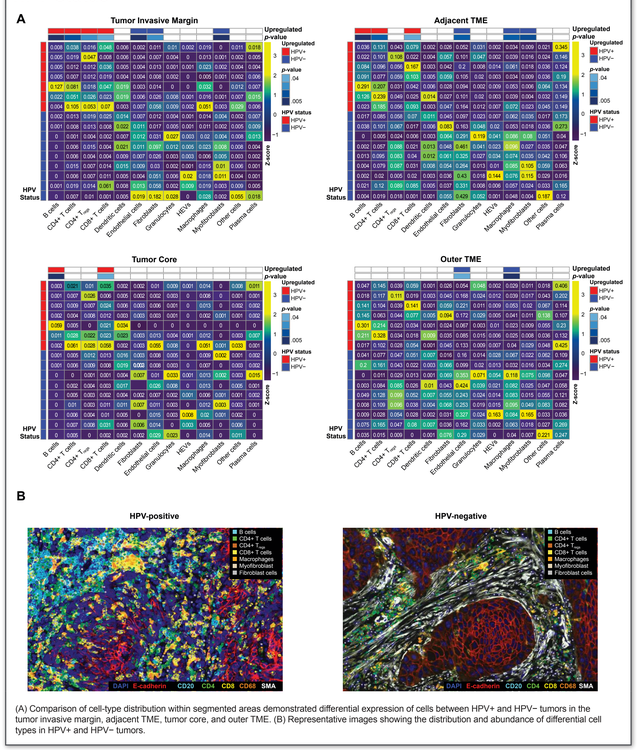

(A) Comparison of cell-type distribution within segmented areas demonstrated differential expression of cells between HPV+ and HPV− tumors in the tumor invasive margin, adjacent TME, tumor core, and outer TME. (B) Representative images showing the distribution and abundance of differential cell types in HPV+ and HPV− tumors.

Differential cell state markers within areas in HPV+ and HPV− tumors

- In the TME of HPV+ tumors, we observed upregulation in CD45RO and CD44 (T-cell memory and activation markers, respectively) while in the HPV− tumors we saw upregulation in myeloid (CD14) and M2 macrophages (CD163) markers
- In the tumor area, CD44+ was upregulated in the HPV− tumors by the tumor cells (stemness marker), while several immune checkpoints (ICOS and IDO1) and activation molecules (CD45RO and Granzyme B) were upregulated in the HPV+ tumors

Figure 6. Differential Spatial Abundance of Immune Cell Status Stratified by HPV Status

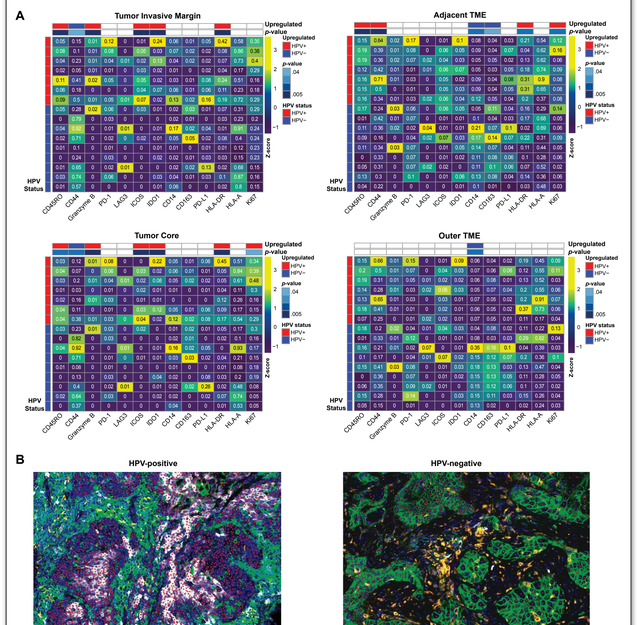

(A) Comparison of cell status markers within segmented areas demonstrated differential expression of cell state markers between HPV+ and HPV− tumors in the tumor invasive margin, adjacent TME, tumor core, and outer TME. (B) Representative images showing the distribution of cell state markers in HPV+ and HPV− tumors.

Spatial analysis reveals differential immune cell interactions in HPV+ and HPV− HNSCC tumors

- For an extended spatial analysis we performed PCA to identify the main sources of variability in the cohort. Interestingly, PC1 strongly separated between HPV+ and HPV− tumors (**Figure 7A–B**)
- PC1 was highly correlated with CD45 positivity in the TME and inversely correlated to fibroblasts abundance
- Differentially expressed spatial features analysis identified CD44+ B cells interactions with CD45RO+ CD4 T cells, IDO1+ tumor cells interactions with HLA-A+ CD8 T cells and double positivity of plasma cells to CD79a and CD31 as the main upregulated features in HPV+ tumors (**Figure 7C**)
- In HPV− tumors, the main upregulated feature was CD44+ positivity within tumor cells

Figure 7. Spatially Resolved Immune Cell Interactions in HPV+ and HPV− HNSCC Tumors

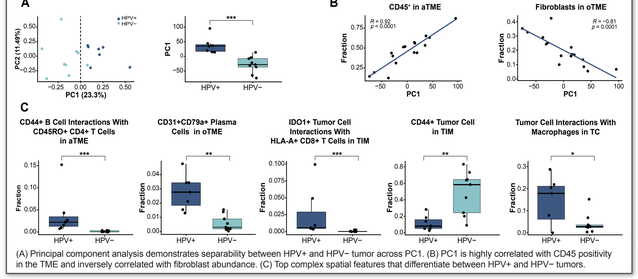

(A) Principal component analysis demonstrates separability between HPV+ and HPV− tumor across PC1. (B) PC1 is highly correlated with CD45 positivity in the TME and inversely correlated with fibroblast abundance. (C) Top complex spatial features that differentiate between HPV+ and HPV− tumors.